International Journal of Engineering, Mathematical and Physical Sciences
ISSN: 2517-9934
Vol:10, No:10, 2016

A Lagrangian Hamiltonian Computational Method for Hyper-Elastic Structural Dynamics

Hosein Falahaty, Hitoshi Gotoh, Abbas Khayyer

***Abstract*—**Performance of a Hamiltonian based particle method in simulation of nonlinear structural dynamics is subjected to investigation in terms of stability and accuracy. The governing equation of motion is derived based on Hamilton's principle of least action, while the deformation gradient is obtained according to Weighted Least Square method. The hyper-elasticity models of Saint Venant-Kirchhoff and a compressible version similar to Mooney-Rivlin are engaged for the calculation of second Piola-Kirchhoff stress tensor, respectively. Stability along with accuracy of numerical model is verified by reproducing critical stress fields in static and dynamic responses. As the results, although performance of Hamiltonian based model is evaluated as being acceptable in dealing with intense extensional stress fields, however kinds of instabilities reveal in the case of violent collision which can be most likely attributed to zero energy singular modes.

***Keywords*—**Hamilton's principle of least action, particle based method, hyper-elasticity, analysis of stability.

I. Introduction

TAKING advantage of Lagrangian formulation, meshfree particle based methods are capable of donating significant contributions to structural dynamics. Absence of rigid connectivity between elements (i.e. grid system) enables particle methods to cope with problems including extremely large deformations where mesh based methods are usually prone to serious problems associated with intense mesh distortion. Specifically, in the case of fragmentation, particle methods are capable of reproducing crack propagation through arbitrary roots, in contrast with the mesh based methods at which the cracks should necessarily happen across the nodes of the element. Thus, in so many studies in the literature, application of particle methods into problems involved in large structural deformations (i.e. nonlinear elasticity and fracture mechanism) has been put forward in recent decades.

Numerous studies have been carried out on application of particle methods into structural dynamics so far, either based on kernel approximations, e.g. Smoothed Particle Hydrodynamics (SPH) [1], [2] and Moving Particle Semi-implicit [3], or based on field approximation, e.g. Element Free Galerkin [4]. In this regard, Libersky and Petschek [5] employed SPH to fracture dynamics. They modeled fragmentation, setting the stress to zero, after yielding a critical threshold of strain. It was revealed that SPH suffers from intrinsic deficiencies, i.e. lack of consistency (which decreases the accuracy) and tensile instability [6], [7].

A variety of efforts were dedicated to remove the aforementioned deficiencies of SPH particle method. Johnson and Beissel [8] attributed the numerical errors involved in the cases of extensional strains to the lack of linear completeness. Randles and Libersky [9] and Krongauz and Belytschko [10] proposed corrections (so called normalization) to the derivatives of stress and displacement fields which enabled them to reproduce either constant or linear fields. The results of these corrections were identical to those of Moving Least Square (MLS) in EFG [11]. Dilts employed MLS approximations into SPH methods [12]-[14].

Swegle et al. [15] explained in details that particle methods suffer from a crucial deficiency, i.e. tensile instability. Belytschko and Xiao [16] performed a comprehensive study on the effect of Eulerian kernels versus Lagrangian kernels with respect to material instability. Based on their results, the tensile instability can be removed by using a Lagrangian kernel.

With regard to MPS, Song et al. [17] employed MPS for simulation of fragmentation in chalk. Kondo et al. [18] and Suzuki and Koshizuka [19] studied the elastic dynamics with special attention to the energy conservation property of elastic body. They derived the motion equations from Lagrangian based on the Hamiltonian's principle of least action, (according to [20]). Employing Lagrangian kernel, the tensile instability was avoided in their model. They also used symplectic scheme for time integration, in order to improve the conservation of energy in the Hamiltonian system. Kondo et al. [21] developed an artificial stabilizing scheme for suppressing the spurious oscillations of particles which were attributed to singular zero energy modes. Khayyer and Gotoh [22] performed a comprehensive stability analysis, describing the criterion for commencement of tensile instability in MPS based pressure calculations, following the approach of swegle [23]. They also proposed enhanced schemes for improvement of the stability and accuracy of the MPS model, e.g. Corrective matrix for more accurate approximation of gradient [24]. Hwang et al. [25] proposed a fully-Lagrangian MPS-based coupled model to the problem of interaction between incompressible fluid and linear elastic structure.

The present study aims to investigate the performance of Hamiltonian based structural model [19] in simulation of nonlinear structural dynamics, in terms of stability and accuracy. The accuracy and stability of the model are examined by reproducing critical stress fields in cases of spurious

Hosein Falahaty (PhD student) is with the Department of Civil and Earth Resources Engineering, Kyoto University, Nishigyo-ku, Kyoto 615-8540, Japan (Phone: +81-75-383-3312, Fax: +81-75-383-3312, e-mail: hosein.falahaty.35z@st.kyoto-u.ac.jp).

Professor Hitoshi Gotoh and Associate Professor Abbas Khayyer are with the Department of Civil and Earth Resources Engineering, Kyoto University, Nishigyo-ku, Kyoto 615-8540, Japan (e-mail: gotoh@particle.kuciv.kyoto-u.ac.jp, khayyer@particle.kuciv.kyoto-u.ac.jp)

material instability in rings, colliding rubber rings, pure tension in slab and finally oscillations of a cantilever plate, and static equilibrium state of a cantilever beam. Lagrangian kernel is used all through the simulations along with the application of hyper-elasticity models of Saint Venant-Kirchhoff and a compressive version similar to Mooney-Rivlin.

II. Governing Equations

Hamiltonian based governing equation of motion for structural analysis is described on the basis of Hamilton's principle of least action as [19]

$$\frac{\partial \boldsymbol{v_i}}{\partial t} = -\frac{1}{\rho_i}\sum_j \frac{\partial \psi_j}{\partial \boldsymbol{r_i}} \tag{1}$$

where, $\boldsymbol{v}$ represents the velocity vector, ψ stands for the strain energy density function, ρ is the density of structural material, $\boldsymbol{r}$ is position vector and subscripts i and j refer to main particle and its neighbors, respectively. Since ψ is solely a function of deformation gradient tensor ($\boldsymbol{F}$) [26], by using the definition of first Piola-Kirchhoff stress tensor $\boldsymbol{\Pi}$, (2), the derivative of stored energy density function ψ with respect to position vector in (1) is transformed into (3):

$$\boldsymbol{\Pi} = \frac{\partial \psi(\boldsymbol{F})}{\partial \boldsymbol{F}} \tag{2}$$

$$\frac{\partial \psi(\boldsymbol{F})}{\partial \boldsymbol{r}} = \frac{\partial \psi(\boldsymbol{F})}{\partial \boldsymbol{F}} : \frac{\partial \boldsymbol{F}}{\partial \boldsymbol{r}} = \boldsymbol{\Pi} : \frac{\partial \boldsymbol{F}}{\partial \boldsymbol{r}} \tag{3}$$

The deformation gradient tensor ($\boldsymbol{F}$) is calculated based on Weighted Least Square method by minimization of the error function in calculation of structural particle positions (4)-(6).

$$\boldsymbol{F}_i = \left(\sum_{j\neq i} \boldsymbol{r}_{ij} \otimes \boldsymbol{r}_{ij}^0 w_{ij}^0\right) \cdot \boldsymbol{A}_i^{-1} \tag{4}$$

$$\boldsymbol{A}_i = \sum_{j\neq i} \boldsymbol{r}_{ij}^0 \otimes \boldsymbol{r}_{ij}^0 w_{ij}^0 \tag{5}$$

$$w_{ij}^0 = \begin{cases} 1 - \dfrac{\left|\boldsymbol{r}_{ij}^0\right|^2}{r_e^2} & \left|\boldsymbol{r}_{ij}^0\right| < r_e \\ 0 & \left|\boldsymbol{r}_{ij}^0\right| \geq r_e \end{cases} \tag{6}$$

With application of (2)-(5), the variational based motion equation is obtained as (7) [19], [21].

$$\frac{\partial \boldsymbol{v}_i}{\partial t} = \frac{1}{\rho_i}\left(\boldsymbol{F}_i \cdot \boldsymbol{S}_i \cdot \boldsymbol{A}_i^{-1} \cdot \sum_{j\neq i} \boldsymbol{r}_{ij}^0 w_{ij}^0 + \sum_{j\neq i} \boldsymbol{F}_j \cdot \boldsymbol{S}_j \cdot \boldsymbol{A}_j^{-1} \cdot \boldsymbol{r}_{ij}^0 w_{ij}^0\right) \tag{7}$$

Here, $\boldsymbol{S}$ is the second Piola-Kirchhoff stress tensor. Indices i and j refer to the main particle and its neighboring particle, respectively.

For time integration, the symplectic scheme [19], [21] is employed as:

$$\begin{aligned} x_i^{n+1} &= x_i^n + v_i^n \Delta t \\ v_i^{n+1} &= v_i^n + \left(\frac{\partial v}{\partial t}\right)_i^{n+1} \Delta t \end{aligned} \tag{8}$$

where, x_i is the i th component ($i = 1, 2$) of position vector $\boldsymbol{r}$, n is the number of time step, and Δt is the magnitude of time step interval.

III. Hyper-Elasticity Models

The second Piola-Kirchhoff stress tensor ($\boldsymbol{S}$) in (7) is obtained from the application of constitutive hyper-elasticity models on Green Lagrange ($\boldsymbol{\varepsilon}$) or Right Cauchy-Green ($\boldsymbol{C}$) strain tensors, (9) and (10):

$$\boldsymbol{\varepsilon} = \frac{1}{2}(\boldsymbol{C} - \boldsymbol{I}) \tag{9}$$

$$\boldsymbol{C} = \boldsymbol{F}^T \cdot \boldsymbol{F} \tag{10}$$

In the present study, two different versions of hyper-elasticity models, i.e. Saint Venant-Kirchhoff (11) and a form of compressible hyper-elasticity model, which roughly resembles Mooney-Rivlin constitutive equation (12) [7] are employed.

$$\psi = \frac{1}{2}\lambda\left[tr\left(\boldsymbol{\varepsilon}\right)\right]^2 + \mu\, tr\left(\boldsymbol{\varepsilon}^2\right) \tag{11}$$

$$\psi = \frac{1}{2}c_1 I_1 + \frac{1}{2}c_2 I_2 - \left[\frac{3}{2}c_1 I_3^{1/3} + \frac{3}{2}c_2 I_3^{2/3} - \frac{\lambda}{4}\left(\ln I_3\right)^2\right] \tag{12}$$

herein, λ and μ are first and second lame constants, respectively. The constants c_1 and c_2 are usually defined according to the results of tension-compression experiments associated with the particular type of material. Also, I_1, I_2 and I_3, represent first, second and third invariants of Cauchy-Green strain tensor ($\boldsymbol{C}$), respectively.

IV. Results and Discussion

In order to investigate the performance of the Hamiltonian based structural model in terms of stability and accuracy, standard benchmark tests, i.e. spurious material instability in rubber ring, colliding rings, slab in pure tension, and finally dynamic response of a cantilever plate [27] and static equilibrium state of a cantilever beam are to be reproduced in this section as follows.

A. Spurious Material Instability in Rubber Ring

The present experiment was first reproduced by Rabczuk et al. [28], in order to explore the onset of spurious instability due to the implementation of Eulerian kernel. In their simulation,

the material constitutive model was assigned as (12) at which c_1=1.265 × 10^5 Pa, c_2=1.012 × 10^4 Pa, λ=1.012 × 10^7 Pa and ρ_s=125.4 kg/m^3 [7]. As the result of their study, it was shown that by using Lagrangian kernel, experiment can be reproduced successfully, while the Eulerian version of kernel will lead to severe distortion of the material.

In this study, a radial pressure field of 6.2×10^4 Pa magnitude was enforced to the inner circumference of the rubber ring. The discretized model consisted of 2201 particles. Fig. 1 indicates the deformation along with radial Cauchy stress ($\sigma_{\theta\theta}$) distribution in rubber ring, at times of t= 0.05 s and t=5 s, simulated by Hamiltonian based model. As can be seen from Fig. 1 (at t = 5 s), the modeled deformation is pure from material instability (i.e. clumping of particles around the circumference of the ring). Also, relatively smooth stress field through the particles of ring during the simulation demonstrates appropriate performance of the Hamiltonian based model (with Lagrangian kernel) in dealing with this stress field [28].

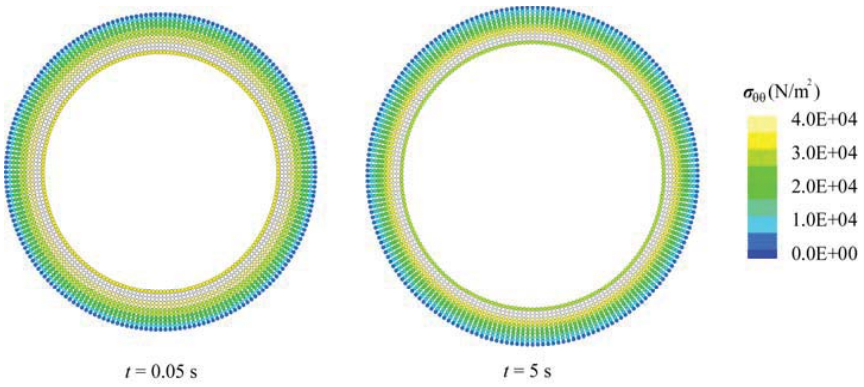

Fig. 1 Deformation along with radial Cauchy stress ($\sigma_{\theta\theta}$) distribution inside the ring due to radial pressure filed enforced on inner circumference

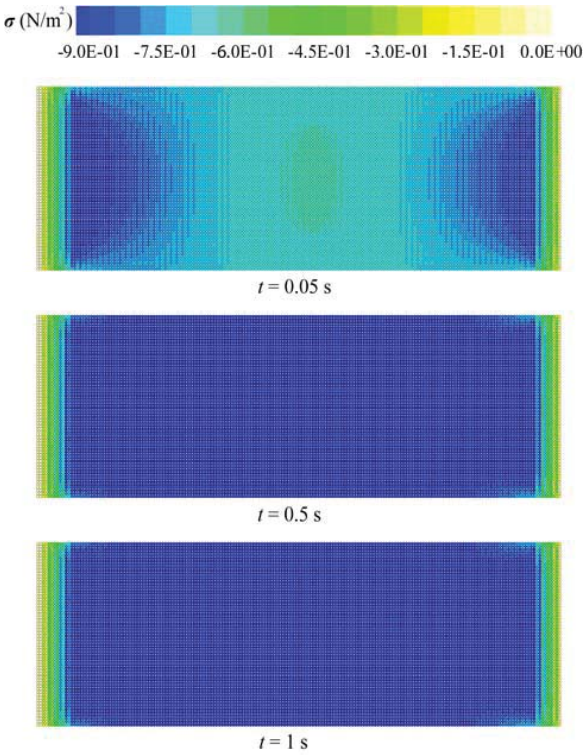

Fig. 2 Extensional stress (Cauchy stress tensor) distribution in slab (pure tension)

B. Pure Tension in Slab

Numerical model was engaged in simulation of a purely extensional stress field. The 3 cm × 1 cm slab model with the total number of particles of 11594 was constructed. The tension was enforced in terms of the acceleration of 0.5 m/s^2 to the particles which were located within 0.2 cm strips off the ends of slab within a time interval of 1 second. The density (ρ_s), bulk (K) and shear (μ) modulus of the material were assigned as 1000 kg/m^3, 3.25×10^6 Pa and 7.15×10^5 Pa, respectively. Saint Venant-Kirchhoff hyper-elasticity model (11) was employed for the calculation of second Piola-Kirchhoff stress tensor.

Fig. 2 demonstrates stress field inside the slab, due to the mentioned extensional stress field. As can be seen in this figure, at t=0.5 s, all the particles except for the region inside the 0.2 cm wide circumferential bands, are subjected to pure extensional stress field without any clumping or violation in the order of particles position.

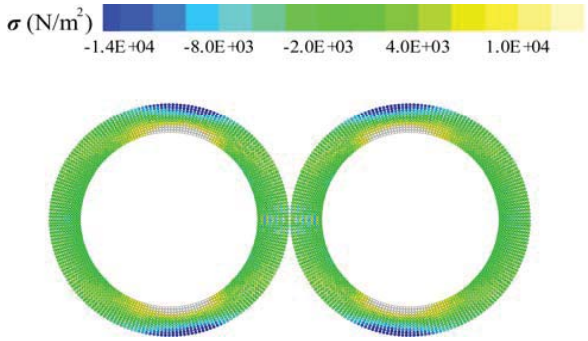

Fig. 3 Deformation and Cauchy stress field (σ) within two rings at the moment of collision

C. Colliding Rubber Rings

Following the verification process, for investigation on the potential of tensile instability, collision of two rubber rings was simulated. The cylindrical arrangement was selected for

particles of the rings with inner and outer diameters of 0.03 cm and 0.04 cm, respectively [27]. Bulk (K) and shear (μ) modulus of the material were adapted as 3.25×10^6 Pa and 7.15×10^5 Pa, respectively. At the initial moment of simulation, the particles of each ring were given an initial velocity of 0.2 m/s directing each other. Saint Venant-Kirchhoff hyper-elasticity model (11) was engaged in modeling of the dynamics. During this collision, circumferential particles (specifically particles neighboring the collision points) of each ring experience intense compressional and extensional stress fields as shown in Fig. 3. As can be seen in Fig. 3, the most critical stress field all through the ring corresponds to the neighboring particles of the collision point. Although, very strong oscillations are happening across the particles of this region, there is no sign of fragmentation, i.e. the structural model has maintained the integrity of the material as a whole [27]. However, severe impact imposed on the particles neighboring the region of collision reveals violations which logically cannot be attributed to the tensile instability. As it is demonstrated in Fig. 3, instabilities are being observed in a region which is affected by strong compressional field. In addition, application of Lagrangian kernel has weakened the hypothesis of material instability in the frame of tensile instability [6]. This kind of violation is more likely to be ascribed to spurious singular oscillations due to zero energy modes [21].

D.Oscillations of a Cantilever Plate

In order to examine the accuracy of the present structural model, the theory of thin oscillating elastic cantilever plate was reproduced [27], [29].

Overall configuration of cantilever plate of interest is shown in Fig. 4. Total length of the plate is 0.24 m, while the outer 0.04 m segment is penetrated into the gap between upper and lower bearings, in order to provide sufficient rigidity at the cantilever support (i.e. l=0.2m, where l is the free length of the plate).

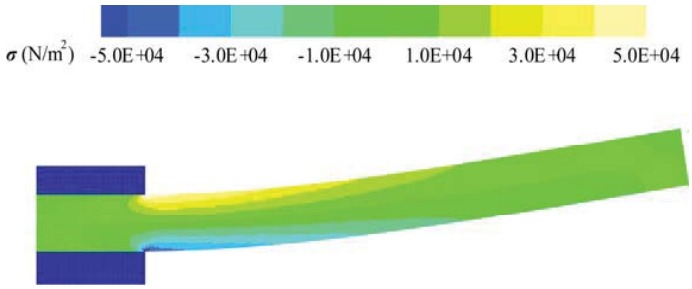

Fig. 4 Deformations and Cauchy stress distribution in oscillating cantilever plate (t = 0.07 s)

The free end of plate is given an initial velocity of v_l = 0.01 m/s perpendicular to the axis of the plate. According to the analytical solution, the initial velocity distribution among the particles of the plate is given as:

$$v_y(x) = v_l c_0 \frac{f(x)}{f(l)} \tag{13}$$

where,

$$f(x) = (\cos kl + \cosh kl)(\cos kx - \cosh kx) + (\sin kl - \sinh kl)(\sinh kx - \sin kx) \tag{14}$$

here, x is the coordinate parallel to the plate axes.

The angular velocity (ω) of oscillation is obtained as:

$$\omega^2 = \frac{EH^2k^4}{12\rho(1-\nu^2)} \tag{15}$$

here, c_0 is the velocity of sound in the material ($c_0 = \sqrt{K/\rho_s}$) and H is the thickness of the plate (=0.02 cm). Bulk (K) and shear (μ) modulus of the rubber material are adjusted as 3.25×10^6 Pa and 7.15×10^5 Pa, respectively. E and ν are modulus of Elasticity and Poisson ratio of the material respectively. Also, k is obtained from (16), while for the fundamental mode of vibration, effective length is as kl = 1.875 [27].

$$\cos(kl)\cosh(kl) = -1 \tag{16}$$

The Saint Venant-Kirchhoff hyper-elasticity model is assigned as the constitutive equation corresponding to material.

The time series of oscillations of free end of the cantilever plate, modeled by the use of the Hamiltonian based structural model is shown in Fig. 5. Also, the dimensionless period and amplitude of the oscillations are compared with analytical solution as well as results of previous studies in Table I. Despite of the fact that numerical simulation is vulnerable to spurious oscillations due to zero energy modes and also concerning that Saint Venant-Kirchhoff is used in this simulation; however, the results of the simulation are in appropriate range compared to the previous studies.

TABLE I
VERIFICATION OF THE DIMENSIONLESS PERIOD AND AMPLITUDE OF THE OSCILLATIONS OF THE FREE END OF THE PLATE

	Dimensionless period	Dimensionless amplitude
Analytical solution	72.39	0.115
Present numerical model	74.38	0.114
Gray et al. [27]	82	0.125
Antoci et al. [30]	81.5	0.126
Rafiee and Tiagarajan [31]	82.2	0.126

E. Static Equilibrium of a Cantilever Beam

A concentrated load of 0.005 N magnitude was imposed to

the free end of a cantilever beam of 0.16 m length and 0.02 m height in y direction.

The particle distance was adjusted as 0.002 m. Young's modulus and Poisson's ratio of the beam material were assigned as 1.0×10^5 Pa and 0.3, respectively.

Fig. 6 demonstrates the deflection of the beam in the state of equilibrium, simulated by the Hamiltonian structural model against analytical solution of the problem. As can be seen, there is well agreement among deflection modeled by the Hamiltonian based structural model and that of analytical solution.

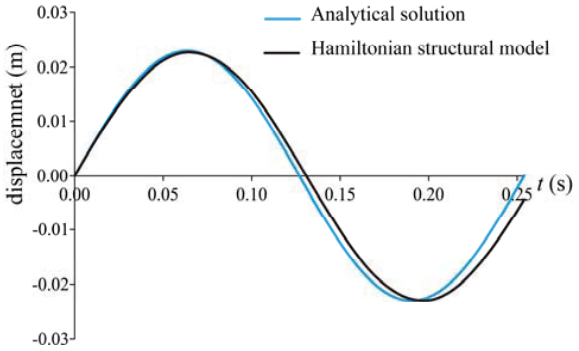

Fig. 5 Time series of displacements of free end of the rubber plate (simulation vs. analytical solution)

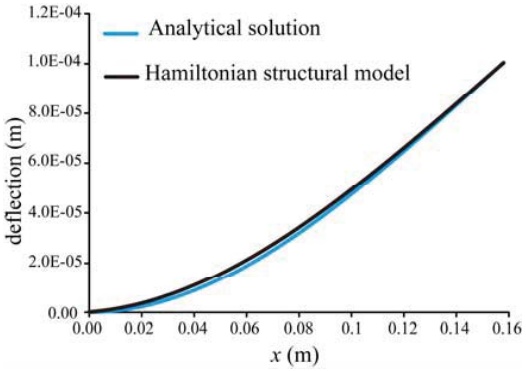

Fig. 6 Deflection of a cantilever beam exposed to concentrated load at the free end (static equilibrium state), simulation vs. analytical solution

V. Conclusion

The aim of the present paper was to investigate the performance of the Hamiltonian based structural model [19] in terms of stability and accuracy. Saint Venant-Kirchhoff and a compressible version similar to Mooney-Rivlin constitutive equations were employed. The stability and accuracy of numerical model were subjected to examination, by reproducing critical stress fields in cases of spurious material instability, colliding rings, slab in pure tension and finally dynamic response of a cantilever plate and static equilibrium state of a cantilever beam.

The stability of the Hamiltonian based model, especially with regard to tensile instability was evaluated well in simulation of cases including spurious material instability in rubber ring and pure tension in the slab.

As the result, the Hamiltonian model is capable of treating well with tensile instability in the mentioned ranges of linear and nonlinear elasticity. However, in the case of colliding rings, local violations in the region of collision were observed which were more likely to be ascribed to zero energy modes rather than tensile instability.

In the case of free oscillating cantilever plate and static equilibrium state of a cantilever beam, the accuracy of the results of model was estimated as being acceptable, almost without any significant instability.

References

[1] L.B. Lucy, "A numerical approach to the testing of fission hypothesis", *Astronom. J.*, vol. 82, 1977, pp. 1013–1024.
[2] R.A. Gingold, J.J. Monaghan, "Smoothed particle hydrodynamics: theory and applications to non-spherical stars", *Mon. Not.R. Astr. Soc.*, vol. 181, 1977, pp. 375–389.
[3] S. Koshizuka and Y. Oka, "Moving particle semi-implicit method for fragmentation of incompressible fluid", *Nuclear Science and Engineering*, vol. 123, 1996, pp. 421-434.
[4] T. Belytschko, Y.Y. Lu, L. Gu, "Element-free Galerkin methods", *Int. J. Numer. Methods Engrg.*, vol. 37, 1994, pp. 229–256.
[5] L.D. Libersky, A.G. Petschek, "Smooth particle hydrodynamics with strength of materials, Advances in the Free Lagrange Method", *Lecture Notes in Physics*, vol. 395, 1990.
[6] T. Belytschko, Y. Guo, W.K. Liu, S.P. Xiao, "A unified stability analysis of meshless particle methods", *Int. J. Numer. Methods Engrg.*, vol. 48, 2000, pp. 1359–1400.
[7] S.P. Xiao, T. Belytschko, "Material stability analysis of particle methods", *Adv. Comput. Math.*, vol. 23, 2005, pp. 171–190.
[8] G.R. Johnson, S.R. Beissel, "Normalized smoothing functions for SPH impact computations", *Int. J. Numer. Methods Engrg.*, vol. 39, 1996, pp. 2725–2741.
[9] P.W. Randles, L.D. Libersky, "Recent improvements in SPH modeling of hypervelocity impact", *Int. J. Impact Engrg.*, vol. 20, 1997, pp. 525–532.
[10] Y. Krongauz, T. Belytschko, "Consistent pseudo derivatives in meshless methods", *Comput. Methods Appl. Mech. Engrg.*, vol. 146, 1997, pp. 371–386.
[11] T. Belytschko, Y. Krongauz, D. Organ, P. Krysl, "Meshless methods: An overview and recent developments", *Comput. Methods Appl. Mech. Engrg.*, vol. 139, 1996, pp. 3–47.
[12] G.A. Dilts, "Moving least squares particle hydrodynamics II: Conservation and boundaries", *Int. J. Numer. Methods Engrg.*, vol. 48, 2000, pp. 1503–1524.
[13] G.A. Dilts, "Moving-least-squares-particle hydrodynamics I: Consistency and stability", *Int. J. Numer. Methods Engrg.*, vol. 44, 1999, pp. 1115–1155.
[14] G.A. Dilts, "Some recent developments for moving-least-squares particle methods", *First M.I.T. Conference on Computational Fluid and Soil Mechanics*, *Preprint, Massachusetts Institute of Technology, Cambridge, MA 02139*, USA, June 12–14, 2001.
[15] J.W. Swegle, S.W. Attaway, M.W. Heinstein, F.J. Mello, Hicks D.L., "An Analysis of Smoothed Particle Hydrodynamics", *Sandia Report SAND93-2513*, 1994, SNL, Albuquerque, NM 87185.
[16] T. Belytschko, S.P. Xiao, "Stability analysis of particle methods with corrected derivatives", *Comput. Math. Appl.*, vol. 43, 2000, pp. 329–350.
[17] M.S. Song, S. Koshizuka, Y. Oka, "A particle method for dynamic simulation of elastic solids", *in Proc. 6th World Congress on Computational Mechanics (WCCM VI)*, Beijing, 5–10 September 2004.
[18] M. Kondo, Y. Suzuki, S. Koshizuka, "Application of symplectic scheme to three-dimensional elastic analysis using MPS method (in Japanese)", *Transactions of the Japan Society of Mechanical Engineers*, vol. 72, 2006, pp. 65–71.
[19] Y. Suzuki, S. Koshizuka, "A Hamiltonian particle method for non-linear elastodynamics", *Int. J. Numer. Methods Engrg.*, 74, 2008, 1344–1373.
[20] J.E. Marsden, T.J.R. Hughes, "Mathematical Foundations of Elasticity", *Prentice Hall: Englewood Cliffs*, NJ, 1983.

[21] M. Kondo, Y. Suzuki and S. Koshizuka, "Suppressing local particle oscillations in the Hamiltonian particle method for elasticity", *Int. J. Numer. Meth. Engng.*, vol. 81, 2010, pp. 1514–1528.
[22] A. Khayyer, H. Gotoh, "Enhancement of stability and accuracy of the moving particle semi-implicit method", *J. Comput. Phys.*, vol. 230, 2011, pp. pp. 3093–3118.
[23] J.W. Swegle, "Conservation of momentum and tensile instability in particle methods", *Sandia Report SAND 2000-1223*, 2000.
[24] J. Bonet, T.S. Lok, "Variational and momentum preservation aspects of smooth particle hydrodynamic formulation", *Comput. Methods Appl. Mech. Engrg.*, vol. 180, 1999, pp. 97–115.
[25] S.C. Hwang, A. Khayyer, H. Gotoh and J.C. Park, "Development of a fully Lagrangian MPS-based coupled method for simulation of fluid-structure interaction problems", *Journal of Fluids and Structures*, vol. 50, 2014, pp. 497-511.
[26] G. A. Holzapfel, "Nonlinear solid mechanics: a continuum approach for engineering", *Meccanica*, vol. 37, 2000, pp. 489-490.
[27] J.P. Gray, J.J. Monaghan, R.P. Swift, "SPH elastic dynamics", *Comput. Meth. Appl. Mech. Engrg.*, vol. 190, 2001, pp. 6641–6662.
[28] T. Rabczuk, T. Belytschko, S.P. Xiao, "Stable particle methods based on Lagrangian kernels", *Comput. Methods Appl. Mech. Engrg.*, vol. 193, 2004, pp. 1035–1063.
[29] L.D. Landau, E.M. Lifshitz, "Theory of Elasticity; Course of Theoretical Physics", *Pergamon Press*, Oxford, vol. 7, 1970.
[30] C. Antoci, M. Gallati, S. Sibilla, "Numerical simulation of fluid–structure interaction by SPH", *Comput. Struct.*, vol. 85, 2007, pp. 879–890.
[31] A. Rafiee, P. K. Thiagarajan, "An SPH projection method for simulating fluid-hypoelastic structure interaction", *Comput. Methods Appl. Mech. Engrg.*, vol. 198, 2009, pp. 2785–2795.